NASA/TP—2001–210989

A Recommended Procedure for Estimating the Cosmic-Ray Spectral Parameter of a Simple Power Law With Applications to Detector Design

L.W. Howell
Marshall Space Flight Center, Marshall Space Flight Center, Alabama

May 2001

The NASA STI Program Office…in Profile

Since its founding, NASA has been dedicated to the advancement of aeronautics and space science. The NASA Scientific and Technical Information (STI) Program Office plays a key part in helping NASA maintain this important role.

The NASA STI Program Office is operated by Langley Research Center, the lead center for NASA's scientific and technical information. The NASA STI Program Office provides access to the NASA STI Database, the largest collection of aeronautical and space science STI in the world. The Program Office is also NASA's institutional mechanism for disseminating the results of its research and development activities. These results are published by NASA in the NASA STI Report Series, which includes the following report types:

- TECHNICAL PUBLICATION. Reports of completed research or a major significant phase of research that present the results of NASA programs and include extensive data or theoretical analysis. Includes compilations of significant scientific and technical data and information deemed to be of continuing reference value. NASA's counterpart of peer-reviewed formal professional papers but has less stringent limitations on manuscript length and extent of graphic presentations.

- TECHNICAL MEMORANDUM. Scientific and technical findings that are preliminary or of specialized interest, e.g., quick release reports, working papers, and bibliographies that contain minimal annotation. Does not contain extensive analysis.

- CONTRACTOR REPORT. Scientific and technical findings by NASA-sponsored contractors and grantees.

- CONFERENCE PUBLICATION. Collected papers from scientific and technical conferences, symposia, seminars, or other meetings sponsored or cosponsored by NASA.

- SPECIAL PUBLICATION. Scientific, technical, or historical information from NASA programs, projects, and mission, often concerned with subjects having substantial public interest.

- TECHNICAL TRANSLATION. English-language translations of foreign scientific and technical material pertinent to NASA's mission.

Specialized services that complement the STI Program Office's diverse offerings include creating custom thesauri, building customized databases, organizing and publishing research results…even providing videos.

For more information about the NASA STI Program Office, see the following:

- Access the NASA STI Program Home Page at ***http://www.sti.nasa.gov***

- E-mail your question via the Internet to help@sti.nasa.gov

- Fax your question to the NASA Access Help Desk at (301) 621–0134

- Telephone the NASA Access Help Desk at (301) 621–0390

- Write to:
  NASA Access Help Desk
  NASA Center for AeroSpace Information
  7121 Standard Drive
  Hanover, MD 21076–1320
  (301)621–0390

NASA/TP—2001–210989

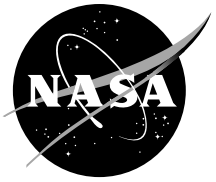

A Recommended Procedure for Estimating the Cosmic-Ray Spectral Parameter of a Simple Power Law With Applications to Detector Design

L.W. Howell
Marshall Space Flight Center, Marshall Space Flight Center, Alabama

National Aeronautics and
Space Administration

Marshall Space Flight Center • MSFC, Alabama 35812

May 2001

Available from:

NASA Center for AeroSpace Information
7121 Standard Drive
Hanover, MD 21076–1320
(301) 621–0390

National Technical Information Service
5285 Port Royal Road
Springfield, VA 22161
(703) 487–4650

TABLE OF CONTENTS

LIST OF FIGURES

LIST OF TABLES

LIST OF ACRONYMS

GCR	galactic cosmic ray
GEANT	“geometry and tracking” Particle Physics Simulation program
ML	maximum likelihood
pdf	probability density function
TP	Technical Publication

NOMENCLATURE

a	intercept in linear mean detector response
b	coefficient in linear mean detector response
c	intercept in linear RMS detector response
d	coefficient in linear RMS detector response
E	random variable symbolizing the energy (units in TeV) of a galactic cosmic ray
L	likelihood function
LL	log-likelihood function
$(\log L)'$	first derivative of the log-likelihood function
$(\log L)''$	second derivative of the log-likelihood function
N_0	average number of events on a given mission
Pr	probability
s	sample standard deviation
u_i	simulated random number from a standard uniform distribution
V	coefficient of variation defined as the standard deviation divided by the mean
Var	variance
Y	Random variable symbolizing the detector's response (energy deposit) (units in GeV)
y_c	cutoff value used to select subsets of detector responses
Z	standard normal random number

NOMENCLATURE (Continued)

∂	partial derivative
α_1	spectral parameter of the simple power law energy spectrum
μ_E	population mean of GCR spectrum
ρ	detector energy resolution
σ_E	population standard deviation of GCR spectrum

TECHNICAL PUBLICATION

A RECOMMENDED PROCEDURE FOR ESTIMATING THE COSMIC-RAY SPECTRAL PARAMETER OF A SIMPLE POWER LAW WITH APPLICATIONS TO DETECTOR DESIGN

1. INTRODUCTION

This Technical Publication (TP) develops and compares two statistical methods for estimating the spectral parameter of the simple power law energy spectrum from simulated detector responses (energy deposits). The maximum likelihood (ML) procedure, which is shown to be the superior approach, is then generalized for application to a set of real cosmic-ray data that make the methodology applicable to existing cosmic-ray data sets.

As part of this research, analytical methods were developed in conjunction with a Monte Carlo simulation to explore the combination of the expected cosmic-ray environment with a generic space-based detector and its planned life cycle. This allows exploration of various detector features and their subsequent impact on estimating this spectral parameter. This study thereby permits instrument developers to make important trade studies in design parameters as a function of the science objectives, which is particularly important for space-based detectors where physical parameters, such as dimension and weight, impose rigorous practical limits to the design envelope.

2. SIMPLE POWER LAW

The simple power law suggests that the number of protons detected above an energy E for an assumed collecting power (combination of size and observing time) is given by[1]

$$N_0(>E) = N_A\left(\frac{E}{E_A}\right)^{-\alpha_1+1} , \tag{1}$$

where E is in units TeV, α_1 is believed to be ≈ 2.8, and N_A and E_A are numbers determined from the detector size and exposure time in the environment. For a typical space-based detector of 1 m^2 with a 3-yr program life, N_A and E_A are 160 and 500 TeV, respectively, implying that this detector is expected to observe 160 proton events above 500 TeV over its expected life cycle. In statistical terms, N_0 is assumed to represent an average number of events while the actual number to be observed on any given mission would follow the Poisson probability distribution with mean number N_0. The number of particles detected depends only on the geometrical factor of the assumed detector and its material composition. The detection efficiency is a convolution of the geometry and material composition and is taken to be independent of energy.

The associated cumulative probability distribution function for E over an energy range $[E_1,E_2]$ is then given by

$$\Phi_0(E) = 1 - \frac{N_0(>E) - N_0(>E_2)}{N_0(>E_1) - N_0(>E_2)} \quad \text{for} \quad E_1 \le E \le E_2$$

$$= 1 - \frac{E^{-\alpha+1} - E_2^{1-\alpha_1}}{E_1^{1-\alpha_1} - E_2^{1-\alpha_1}} \ . \tag{2}$$

Thus, the corresponding probability density function (pdf) for E is obtained by differentiating equation (2) to give

$$\phi_0(E) = \frac{d\Phi_0(E)}{dE}$$

$$= \frac{\alpha_1 - 1}{E_1^{1-\alpha_1} - E_2^{1-\alpha_1}} E^{-\alpha_1} \quad \text{for} \quad E_1 \le E \le E_2 \ . \tag{3}$$

To randomly sample GCR proton event energies from the simple power spectrum over the interval $[E_1,E_2]$, $u_i=\Phi_0(E_i)$ is solved in terms of E_i to obtain

$$E_i = \Phi_0^{-1}(u_i) = \left[E_1^{1-\alpha_1} + u_i\left(E_2^{1-\alpha_1} - E_1^{1-\alpha_1}\right)\right]^{\frac{1}{1-\alpha_1}} , \tag{4}$$

where u_i is a simulated random number from a standard uniform distribution and $\Phi_0{}^{-1}$ represents the inverse function of Φ_0, which is a conventional notation that will be used in subsequent sections. The mean, variance, and other moments of the simple power law distribution are determined by the expected value operator, where the general form of $\left\langle E^m \right\rangle$ is

$$\begin{aligned} \left\langle E^m \right\rangle &= \int_{E_1}^{E_2} E^m \phi_0(E) dE \\ &= \left(\frac{\alpha_1 - 1}{\alpha_1 - m - 1} \right) \frac{E_1^{m+1-\alpha_1} - E_2^{m+1-\alpha_1}}{E_1^{1-\alpha_1} - E_2^{1-\alpha_1}} \ . \end{aligned} \tag{5}$$

Note a crucial point at this time, and that is $<E^2>$ becomes infinite (as do all other higher moments) as E_2 goes to infinity, which is easily seen in equation (6):

$$\lim_{b\to\infty} \int_a^b x^2 x^{-\lambda}\, dx = \infty \text{ for all } \lambda \le 3 \text{ and } a > 0 \ . \tag{6}$$

This observation suggests the need for a careful look at the effects of the large variance and other higher moments associated with all power law distributions, even when E_2 is kept finite. A measure of the relative dispersion of the energies of the incident protons, which is independent of units, is defined by $V=\sigma_E/\mu_E$ for the simple power law and is called the coefficient of variation in the statistical literature. An important concept in detector design is the energy resolution ρ of the detector that provides a measure of the relative accuracy of a cosmic-ray detector, which is the fractional error in measurements of a monoenergetic beam. The resolution ρ is defined as the standard deviation divided by the mean response with typical values of 30 to 40 percent.

As will be shown in this TP, the precision with which the spectral parameter α_1 can be estimated from a set of detector responses (energy deposits), measured in terms of its standard deviation, is a function of both the variance of the incident energies and the uncertainty induced by the detector. The dominating component of this measurement precision will be shown to be attributable to the standard deviation of the incident energies σ_E, which in turn can only be controlled through collecting power. Since V and ρ are dimensionless and provide a measure of relative dispersion for the power law distribution and detector, respectively, an instructive comparison will show that $V \gg \rho$. To illustrate these points, a detector life cycle having parameters N_A = 160 and E_A = 500 TeV will observe 52,200 events on average in the energy range E_1 = 20 TeV to E_2 = 5,500 TeV from a simple power law

spectrum when α_1 is 2.8. This gives a mean galactic cosmic-ray (GCR) event energy μ_E = 44.5 TeV, a standard deviation σ_E = 74.10 TeV, and a coefficient of variation V = 166.5 percent. In comparison, the resolution ρ of most detectors is between 30 and 40 percent. E_2 is chosen for this detector life cycle combination as 5,500 TeV, since the expected number of events above this energy are negligible, while E_1 is taken to be 20 TeV for purposes of this discussion.

Since the number of events and their incident energies will vary because of the finite detector size and exposure time, the statistical behavior of the GCR event energies in combination with a detector having energy resolution ρ and the subsequent spectral parameter estimate over multiple missions shall be studied. Thus, for each mission, a random number N of GCR events from a Poisson distribution with mean 52,200 representing the number of simulated events that the detector will observe in the energy range 20 to 5,500 TeV on any given mission is first generated.

Next, the incident energy of each of these N events using equation (4) is simulated. For example, for one such simulated mission, N = 51,883 and the mean and standard deviation of the simulated GCR incident energies are calculated to be 43.85 and 66.39 TeV, respectively. To illustrate the large fluctuations associated with power law distributions, the same number of events (51,883) from a normal distribution having a mean of 44.5 and standard deviation 74.1 so as to match the power law's mean and standard deviation for this energy range when α_1 = 2.8 was also simulated. The sample mean and standard deviation, 44.51 and 74.17, respectively, for a single sample mission, which are much closer to the population mean and variance than those from the power law random samples, were also observed. The process is repeated for 100 missions and the standard deviation for each mission is plotted in figure 1.

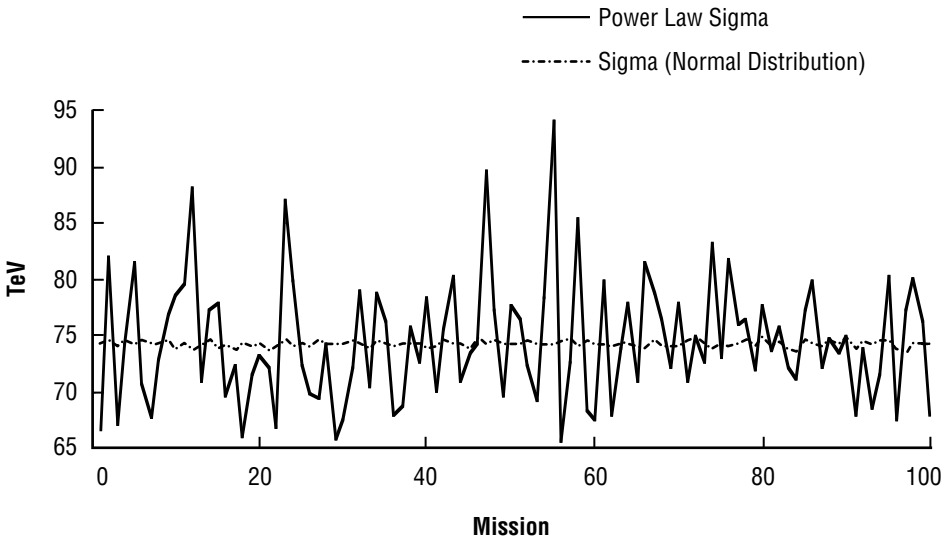

Figure 1. Standard deviation of simulated incident energies from power law (ragged curve) for 100 missions compared with that from normal distribution having same mean and variance.

Note the large fluctuations of the standard deviations for the power law samples from mission to mission; while in contrast, the standard deviations of missions generated from a normal distribution are very stable. As will be seen in subsequent sections, this is why the variation in detector responses is dominated by the variation of the GCR event energies, relative to the uncertainty induced by detector resolution. This in turn contributes the dominant component of the standard deviation of the spectral parameter estimator.

The variation of the sample standard deviation s used as an estimator of σ and measured by its standard deviation is given by

$$\sigma_s = \sqrt{\frac{\mu_4 - \mu_2^2}{4\mu_2 N}} \quad , \tag{7}$$

where μ_r is the rth central moment about the mean,[2] defined for the simple power law as

$$\mu_r = \int (E - u_E)^r \phi_0(E) dE \quad . \tag{8}$$

Thus, the large variation in mission standard deviations is due to the term μ_4, which again is only finite by setting E_2 to a finite value, but nevertheless is responsible for the erratic behavior of the mission-to-mission sample standard deviations depicted in figure 1. This erratic behavior of the observed mission standard deviations will be true for any power law having spectral index α_1 in the range $3 < \alpha 1 \leq 5$. Note that for the normal distribution,

$$\sigma_s = \frac{\sigma}{\sqrt{2N}} \quad , \tag{9}$$

and evaluation of these two formulae yield $\sigma_s = 5$ TeV for the simple power law and 0.229 TeV for the normal distribution, which is roughly a factor of 22.

3. ESTIMATION OF THE SPECTRAL PARAMETER α_1

Of particular interest in the study of cosmic rays is the estimation of the spectral parameter α_1 from a set of data. In this section, two statistical procedures for estimating α_1 are developed and compared. Even though in practice the actual incident particle energies are never observed (but only a measure of their energy deposition from their passage through the detector), it is important to consider the concept of an ideal detector having zero resolution. Thus, such a detector would measure the GCR event energies exactly.

3.1 Method of Moments

The method of moments consists of equating the sample moments with the population moments, which in general leads to k simultaneous nonlinear algebraic equations in the k unknown population parameters. For the simple power law, there is only one parameter to be estimated, so the sample mean $\overline{E}$ is set to the population mean μ_E obtained by setting $m = 1$ in equation (5) to obtain equation (10) to be solved in terms of $\hat{\alpha}_1$:

$$\overline{E} = \left(\frac{\hat{\alpha}_1 - 1}{\hat{\alpha}_1 - 2}\right)\frac{E_1^{2-\hat{\alpha}_1} - E_2^{2-\hat{\alpha}_1}}{E_1^{1-\hat{\alpha}_1} - E_2^{1-\hat{\alpha}_1}} \quad . \tag{10}$$

Thus, for a given sample of size N, this equation is solved in terms of $\hat{\alpha}_1$ by numerical methods to provide an estimate of α_1. This estimator, which is a function of the random variable $\overline{E}$, has its own associated pdf. Since the GCR incident energy E has mean μ_E and finite variance σ_E^2 (only because the upper energy E_2 is finite), it is known by the central limit theorem that the distribution of the sample average $\overline{E}$ follows a normal distribution with mean μ_E and variance σ_E^2/N.

For example, when $\alpha_1 = 2.8$, $E_1 = 20$ TeV, and $E_2 = 5{,}500$ TeV, $\overline{E}$ is normally distributed with mean 44.5 TeV and standard deviation (74.1 TeV)/$N^{1/2}$. These results can be used to obtain the probability distribution of the estimator by solving the probability equation,

$$\Pr\left\{\frac{\left(\frac{\hat{\alpha}_1 - 1}{\hat{\alpha}_1 - 2}\right)\frac{E_1^{2-\hat{\alpha}_1} - E_2^{2-\hat{\alpha}_1}}{E_1^{1-\hat{\alpha}_1} - E_2^{1-\hat{\alpha}_1}} - 44.5}{\frac{74.1}{\sqrt{N}}} \le Z\right\} = \int_{-\infty}^{Z} \frac{1}{\sqrt{2\pi}} e^{-\frac{x^2}{2}}\, dx \quad , \tag{11}$$

in terms of $\hat{\alpha}_1$ for various values of Z. Letting Z vary from –4.7 to 4.7 and setting N = 52,000 events gives the probability distribution of $\hat{\alpha}_1$ shown in figure 2. Also depicted in figure 2 is the relative frequency histogram of the estimates $\hat{\alpha}_1$, based on 5,000 simulated missions. For each mission, 52,000 events on average are simulated and the estimate of α_1 obtained by solving equation (11). Furthermore, even though there is no explicit mathematical form for the pdf, its mean and standard deviation can be calculated by numerical methods. For the distribution shown here, its mean is numerically evaluated to be 2.800 and standard deviation as 0.0115 when N = 52,000, which compares to the mean and standard deviation of the 5,000 simulated estimates with 2.800 and 0.0114, respectively. With the ability to numerically construct this estimator's pdf and moments, the important result found was that its variance is inversely proportional to the sample size N, which happens to be true for many common estimators (e.g., the sample mean, standard deviation, and median). For example, if the number of events is doubled, then the variance is halved; and if the number of events is halved, then the variance doubles. Note that this relationship between sample size and the standard deviation of the estimator $\hat{\alpha}_1$ is based on keeping E_1 and E_2 fixed, so that in practice, increasing the collecting power can reduce the variance.

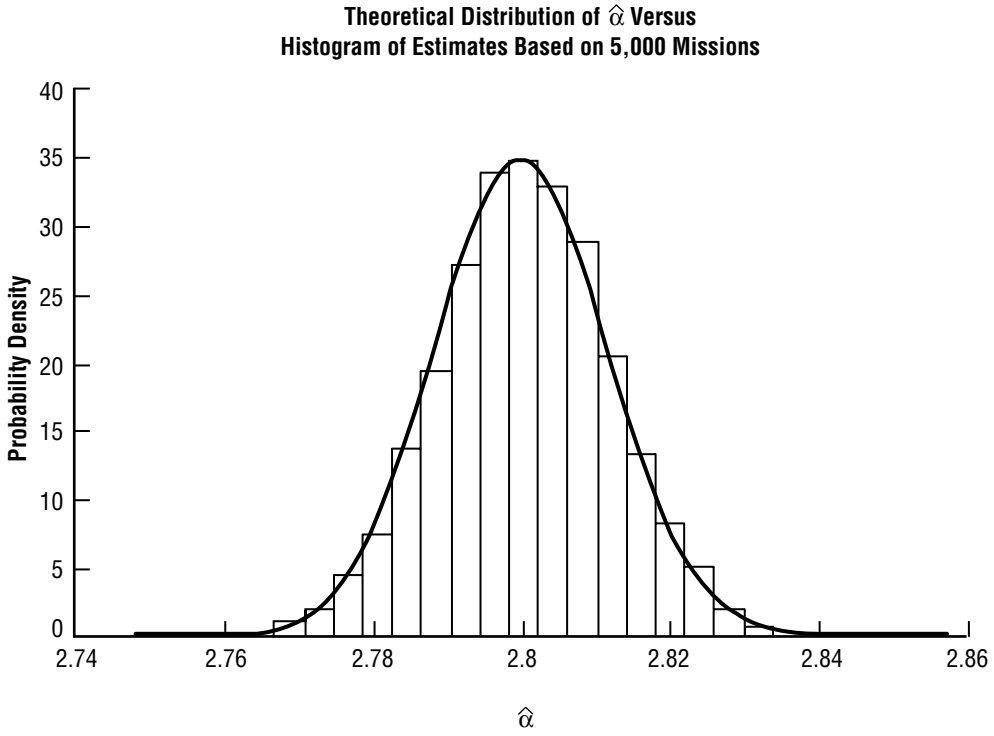

Figure 2. Probability distribution of method of moments estimate of α_1 with relative frequency histogram of spectral parameter estimates obtained from simulation.

3.2 Method of Maximum Likelihood

The likelihood function of a random sample from the simple power law, regarded as a function of the single unknown parameter α_1, is

$$L(\alpha_1) = \left(\frac{\alpha_1 - 1}{E_1^{1-\alpha_1} - E_2^{1-\alpha_1}} \right)^N \left(\prod_{i=1}^{N} E_i \right)^{-\alpha_1} \quad , \quad E_1 \le E_i \le E_2 \ . \tag{12}$$

The method of ML seeks as the estimate of α_1 that value (say, α_{ML}) which maximizes the likelihood function so that $L(\alpha_{\mathrm{ML}}) \ge L(\alpha_1)$ for all α_1. Statistically, this means that the ML estimator leads us to a choice of α_1 that maximizes the probability of obtaining the observed data. In practice, it is often simpler to work with the logarithm of the likelihood function and seek solutions of $(\log L)' = 0$ for which $(\log L)'' < 0$ (indicating a maximum), where the prime and double prime indicate the first and second derivative, respectively. Thus, equation (13) is numerically solved in terms of α_1 to obtain the ML estimate α_{ML}:

$$\frac{\partial \log L}{\partial \alpha_1} = \frac{N}{\alpha_1 - 1} - N \left[\frac{\left(\log E_1\right) E_1^{1-\alpha_1} - \left(\log E_2\right) E_2^{1-\alpha_1}}{E_1^{1-\alpha_1} - E_2^{1-\alpha_1}} \right] - \sum_{i=1}^{N} \log E_i = 0 \ . \tag{13}$$

The second derivative of the log-likelihood function is next obtained. Note that $(\log L)'' < 0$ for all α_1, indicating that $\log L$ is concave; hence, there is a unique maximum, which was graphically observed by plotting $\log L$ as a function of α_1:

$$\frac{\partial^2 \log L}{\partial \alpha_1^2} = -N \left(\frac{1}{(\alpha_1 - 1)^2} + \left[\frac{E_2^{1+\alpha_1} E_1^{1+\alpha_1} \left(\log E_2 - \log E_1\right)^2}{(E_2 E_1^{\alpha_1} - E_1 E_2^{\alpha_1})^2} \right] \right) . \tag{14}$$

By the Cramer-Rao inequality, the lower bound of the variance of any estimator $\hat{\alpha}$ of α_1 is given by

$$\mathrm{Var}(\hat{\alpha}) \ge \frac{-1}{\dfrac{\partial^2 \log L}{\partial \alpha_1^2}} \ , \tag{15}$$

which is asymptotically attained by the ML estimator. Also note that it is inversely proportional to the number of events N as was the variance of the estimator obtained using the method of moments. Other important properties of ML estimators are that they are (1) asymptotically normally distributed and (2) consistency or asymptotically unbiased. Thus, a key question is, "For what values of N are these asymptotic properties achieved by the ML procedure?"

Based on the same 5,000 mission set discussed in section 3, the mean and standard deviation of the 5,000 ML estimates are 2.800 and 0.00782, respectively. Using equations (15) and (16), the Cramer-Rao bound is computed to be 0.00786 when N = 52,000 and α_{ML} = 2.800, which compares very well with the simulation results. Furthermore, the frequency histogram of these 5,000 ML estimates resembled the normal distribution as stated in (1) of the above paragraph. A separate simulation study was conducted in which the sample size N was gradually reduced from 52,000 to 200 and the two asymptotic properties—attaining the Cramer-Rao bound and consistency—were achieved by the ML estimates until N equals $\approx$2,000. A bias on the high side of α_{ML} and failure to attain the Cramer-Rao bound became more and more evident as the number of events N diminished from 2,000 to 200.

Another very important comparison is the ratio of the standard deviation of α_{ML} to that of the estimator, obtained using the method of moments. Direct calculation shows this ratio is roughly 1.45, implying that the ML procedure is significantly better than the method of moments when dealing with the simple power law. This result is not too surprising, however, because ML estimators in general have better statistical properties than the estimators obtained by the method of moments.[3]

4. DETECTOR RESPONSE FUNCTION

Based on GEANT simulations of energy deposition for monoenergetic protons at specified energies of 0.1, 1, 10, 100, 1,000, and 5,000 TeV, the Gaussian distribution provided a reasonable description of the distribution of energy depositions at each of these incident energies.[4] Furthermore, the mean detector response was well approximated by a linear function of incident energy in the range of interest for this study, typically between 10 and 5,500 TeV. Other detector response functions, such as a gamma distribution and another response function constructed from a combination of normal distributions having different parameters, will also be presented.

The random variable Y is introduced to represent the detector's response in terms of energy deposition of a GCR proton of incident energy E. The conditional mean response and standard deviation of Y for a particular incident energy E are modeled as $\mu_{Y|E} = (a + bE)$ and $\sigma_{Y|E} = (c + dE)$, respectively, where the four coefficients a, b, c, and d are estimated using linear regression in the GEANT simulation results. Thus, for each simulated incident GCR proton energy E_i, the detector response is simulated as

$$Y_i = \mu_{Y|E_i} + \sigma_{Y|E_i} Z_i \tag{16}$$

or

$$Y_i = (a + bE_i) + (c + dE_i) Z_i \ , \tag{17}$$

with the nonnegativity constraint $Y_i > 0$ and where Z_i is a standard normal random number having zero mean and unit standard deviation. Thus, the detector response function is defined as

$$g(y \mid E) = \frac{\eta_{y|E}}{\sqrt{2\pi\sigma_{y|E}^2}} e^{-\frac{(y-\mu_{y|E})^2}{2\sigma_{y|E}^2}} \ , \quad y > 0 \ , \tag{18}$$

where $\eta_{y|E}$ is a normalizing coefficient related to the truncation of the normal distribution resulting from the constraint $y > 0$. It is worth noting for constant resolution studies in which a Gaussian response function is assumed and $\rho = \sigma/\mu$ is set to values 0.4 and 0.6, the corresponding detector energy resolution is 39 and 51 percent, respectively, and is rounded to 40 and 50 percent in the figures and tables in this TP.

Thus, $\eta_{y|E}$ is determined from

$$\frac{1}{\eta_{y|E}} = \int_{\frac{-1}{\rho_{y|E}}}^{\infty} \frac{1}{\sqrt{2\pi}} e^{-\frac{z^2}{2}} dz \ , \tag{19}$$

where the lower limit of integration is –1 divided by the resolution function, given as

$$\rho_{y|E} \ = \ \sigma_{Y|E} \ / \mu_{Y|E} \ = \ (c + dE) / (a + bE) \ . \tag{20}$$

First, it is worthwhile to consider a detector having energy resolution $\rho_{y|E} \ = \sigma_{Y|E} \ / \mu_{Y|E}$ a constant ρ and independent of the cosmic-ray's energy E so that $\sigma_{Y|E} = \rho \ \mu_{Y|E}$, where typical values of interest for ρ are 0, 0.2, 0.3, 0.4, and 0.6. It should also be noted that the normalizing coefficient η in equation (19) is constant whenever the detector resolution ρ is energy independent.

Second, a case where $\mu_{Y/E}$ and $\sigma_{Y/E}$ are linear but their ratio is not a constant, so that the detector's resolution is a nonlinear function of incident energy E, was investigated. For this second scenario, two studies were conducted in which the resolution is getting better, from 40-percent resolution at 20 TeV to 30-percent resolution at 5,500 TeV, and then getting worse, from 30-percent resolution at 20 TeV to 40-percent resolution at 5,500 TeV. These two energy-dependent cases are presented in section 8.

5. PROBABILITY DISTRIBUTION OF THE DETECTOR RESPONSE

The probability distribution for the detector response in the presence of the simple power law energy spectrum over the energy range $[E_1,E_2]$ is

$$g_0(y;\alpha_1) = \int_{E_1}^{E_2} g(y \mid E;\rho)\, \phi_0(E;\alpha_1) dE\,, \quad y > 0\ . \tag{21}$$

The spectral parameter α_1 has been explicitly included in the argument list of both the simple power law pdf as $\phi_0(E;\alpha_1)$ and the detector response distribution $g_0(y;\alpha_1)$ in equation (21) to indicate that this spectral index is inherited through the integral.

6. IDEAL DETECTOR

The concept of a zero-resolution or ideal detector is very useful because it sets an upper bound on the expected performance of any real detector. Furthermore, it allows quantifing the magnitude of the uncertainty in the estimate of the spectral parameter. This uncertainty is measured in terms of the standard deviation of the estimator and attributable to event statistics (statistical fluctuation of incident GCR proton energies) relative to the uncertainty in measuring the spectral parameter estimate induced by the detector's nonzero energy resolution.

Thus, for an ideal detector, $\rho = 0$ so that the standard deviation $\sigma_{Y|E} = 0$ for all GCR event energies E. Hence, the detector response to a GCR of energy E is given by $Y = a + bE$ so that the incident energies may be directly obtained as $E = (Y - a)/b$ so that the estimation procedures developed in sections 4 and 5 apply.

6.1 Method of Moments for a "Real" Detector

The conditional expected value theorem is utilized that says the expected value of the conditional expected value is the unconditional expected value,[5] or in the notation of mathematical expectation applied to the detector response Y,

$$\mu_Y = < Y > = \ll Y \mid E \gg \quad . \tag{22}$$

Thus, for a detector with constant resolution ρ, the following is obtained:

$$\mu_Y = (a + b\mu_E)\left[1 + \rho\eta(\rho) \int_{-1/\rho}^{\infty} \frac{x}{\sqrt{2\pi}} e^{-\frac{x^2}{2}} dx\right] , \tag{23}$$

where μ_Y is the mean of the detector response distribution and μ_E is the mean of the simple power law distribution. The term involving the integral can be thought of as a correction term to the mean for the truncation and can be ignored whenever $\rho < 0.30$; i.e., 30-percent resolution or better. Using the method of moments, μ_Y is estimated with the sample average $\bar{Y}$. When combined with equation (5) with $m = 1$ for μ_E yields equation (24) that can then be solved in terms of $\hat{\alpha}_1$ by numerical methods:

$$\frac{\bar{Y}/b}{\left[1+\rho\eta(\rho)\int_{-1/\rho}^{\infty}\frac{x}{\sqrt{2\pi}}e^{-\frac{x^2}{2}}dx\right]}-\frac{a}{b}=\left(\frac{\hat{\alpha}_1-1}{\hat{\alpha}_1-2}\right)\frac{E_1^{2-\hat{\alpha}_1}-E_2^{2-\hat{\alpha}_1}}{E_1^{1-\hat{\alpha}_1}-E_2^{1-\hat{\alpha}_1}}\ . \tag{24}$$

For example, when the resolution is a constant 40 percent ($\rho = 0.40$), the point estimate of the spectral parameter α_1, based on the 5,000 missions, is 2.801 using equation (24) and 2.79 using the same equation but with the correction term set to zero in the denominator. This results in a bias of ≈ 0.01 that can be removed by including this correction term. This effect is much more pronounced when $\rho = 0.6$ and results in a bias of 0.1 in the point estimate of α_1, so the correction term is critical.

When the detector response distribution is symmetric and truncation is negligible so that $\mu_Y = (a + b\mu_E)$, then α_1 can always be estimated using the mean of the detector responses $\bar{Y}$ to estimate μ_Y in equation (5) with $m = 1$. This implies that knowledge of the variance of the detector distribution, and hence the resolution, is not required in order to estimate α_1, provided it is known the resolution is <30 percent so the effect of truncation can be ignored.

This is a useful result because if the uncertainty regarding the true resolution is non negligible, then the method of moments might be a good way to proceed with the estimation of α_1; e.g., it is known the detector's energy resolution is <30 percent but nothing more. However, as already noted, the method of moments does not provide the minimum variance estimator that the ML method does, which requires a complete specification of the detector parameters *a, b, c*, and *d* of this assumed Gaussian response function. Furthermore, the energy resolution of most real detectors is worse than 30 percent.

This estimator, based on the method of moments, is a function of the random variable *Y* and has its own associated pdf. Since *Y* has mean μ_Y and variance σ_Y^2, it is known by the central limit theorem the distribution of $\bar{Y}$ follows a normal distribution with mean μ_Y and variance σ_Y^2/N. Thus, the variance of the detector response *Y* is $\sigma_Y^2 = \langle Y^2 \rangle - \mu_Y^2$ where

$$\langle Y^2 \rangle = \left(a^2 + 2ab\mu_E + b^2\sigma_E^2 + b^2\mu_E^2\right)\eta(\rho)\left[\int_{-1/\rho}^{\infty}\frac{(1+\rho x)^2}{\sqrt{2\pi}}e^{-\frac{x^2}{2}}dx\right]. \tag{25}$$

For example, when $\alpha_1 = 2.8$, $E_1 = 20$ TeV, $E_2 = 5{,}500$ TeV, and $\rho = 0.40$, $\bar{Y}$ is normally distributed with mean 131.58 GeV and standard deviation (213.69 GeV)/$N^{1/2}$. The probability distribution of $\hat{\alpha}_1$ can be constructed and its mean and standard deviation obtained by solving the probability equation in equation (26) using the methods discussed with equation (11):

$$\Pr\left\{\frac{\left[a+b\left(\frac{\hat{\alpha}_1-1}{\hat{\alpha}_1-2}\right)\frac{E_1^{2-\hat{\alpha}_1}-E_2^{2-\hat{\alpha}_1}}{E_1^{1-\hat{\alpha}_1}-E_2^{1-\hat{\alpha}_1}}\right]\left[1+\rho\eta(\rho)\int_{-1/\rho}^{\infty}\frac{x}{\sqrt{2\pi}}e^{-\frac{x^2}{2}}dx\right]-131.58}{\frac{213.69}{\sqrt{N}}}\le Z\right\}=\int_{-\infty}^{Z}\frac{1}{\sqrt{2\pi}}e^{-\frac{x^2}{2}}dx. \quad (26)$$

If the truncation effect is negligible in equation (25), then the following succinct formula for the variance of the detector response as a function of detector parameters a, b, and ρ and the mean μ_E and variance σ_E^2 of the power law distribution is obtained:

$$\sigma_y^2 = b^2\sigma_E^2 + \rho^2\left[\left(a+b\mu_E\right)^2 + b^2\sigma_E^2\right] . \quad (27)$$

In terms of the standard deviation of the detector response σ_y, the approximation in equation (27) is seen to be quite good. When $\rho = 0.4$, this formula yields $\sigma_y = 213.37$ GeV as compared to the exact value of 213.69 GeV obtained from equation (26) using the integral correction terms. When $\rho = 0.6$, this approximation yields $\sigma_y = 237.31$ GeV as compared to the actual value of 239.78 GeV. Thus, ignoring the truncation is not too serious when estimating the standard deviation but can be devastating for $\rho > 0.4$ when estimating the mean μ_Y and hence α_1 when using the method of moments. Much insight into the estimation of the spectral parameter α_1 can be gleaned from equation (27) as it shows the relationship between the variance σ_Y^2 of the detector response distribution, the variance σ_E^2 of the GCR proton energy spectrum, and the detector response function parameters a, b, and ρ.

The influence of the variance and other higher moments of the simple power law energy spectrum is visualized in figure 3, which shows the mean detector response (mean energy deposit) per mission for 30 simulated missions in comparison with the mean incident proton energy for 30 missions. Corresponding standard deviations per mission are plotted in figure 4. Note that the detector response mean and standard deviation per mission tends to track the mean and standard deviation of the incident energies for the 30 missions, illustrating the strong influence of the GCR energy mission-to-mission fluctuations on the detector response variation, even in the presence of the "smearing" induced by this detector having 40-percent energy resolution. In section 6.2, the component of variation due to the GCR event statistics will be the dominating the component of the total variation in the standard deviation of the estimator of the spectral index α_1.

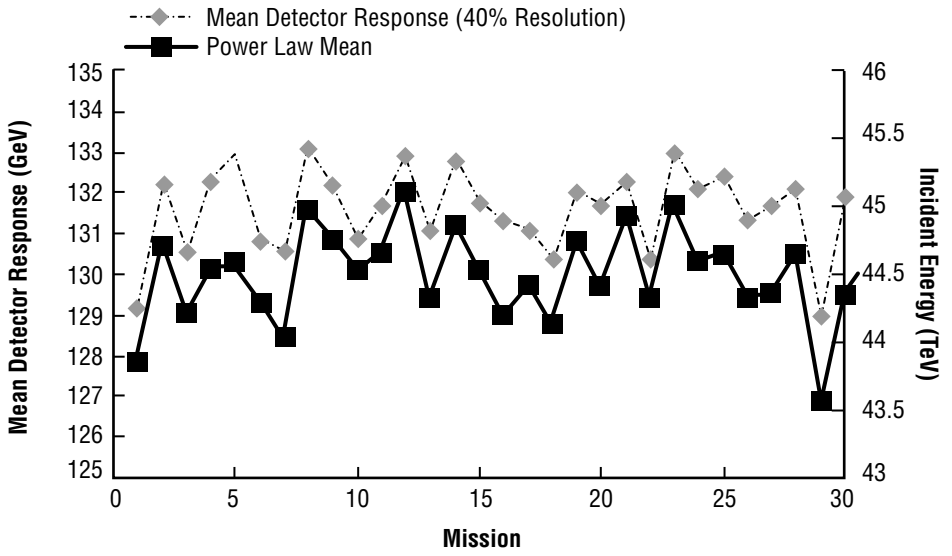

Figure 3. Comparing the mean incident energy with the mean of the detector responses for each of 30 missions.

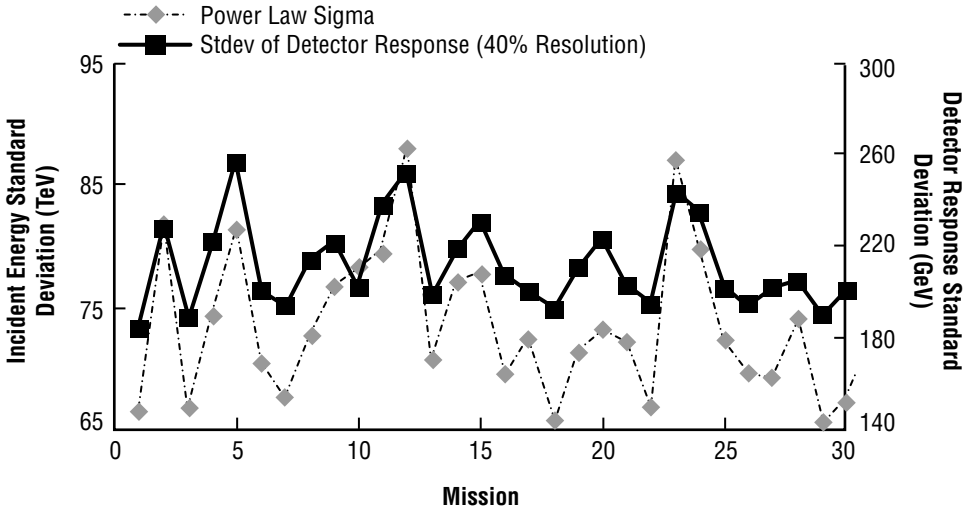

Figure 4. Comparing the standard deviation of the GCR incident energies with the standard deviation of the detector responses for each of 30 missions.

6.2 Maximum Likelihood for a "Real" Detector

As in section 6.1, the method of ML seeks α_{ML} which maximizes the log-L function so that log $L(\alpha_{\mathrm{ML}}) \geq \log L(\alpha_1)$ for all α_1, where the likelihood function for the detector response in the presence of the simple power law energy spectrum of N incident GCR protons over the energy range $[E_1,E_2]$ is

$$\log L(\alpha_1) = \sum_{j=1}^{N} \log\left[\left(g_0(y_j;\alpha_1)\right)\right] = \sum_{j=1}^{N} \log\left[\int_{E_1}^{E_2} g(y_j \mid E)\, \phi_0(E;\alpha_1) dE\right] . \tag{28}$$

Because of the complexity of the integral and the desired capability to easily change the functional form of the detector response function g in equation (28), a numerical minimization algorithm called the Nelder-Mead downhill simplex method that does not require gradient information (derivatives) for obtaining α_{ML} was chosen.[6] Since this is a minimization algorithm, the objective function is defined as

$$O(\alpha_1) = -\log L(\alpha_1) = -\sum_{j=1}^{N} \log\left[\int_{E_1}^{E_2} g(y_j \mid E)\, \phi_0(E;\alpha_1) dE\right] , \tag{29}$$

so that minimizing $O(\alpha_1)$ maximizes log $L(\alpha_1)$ as desired, where the integral is numerically evaluated. The following two termination criteria are used to halt the search procedure for the ML estimate at the $(m + 1)$th iteration:

$$\begin{aligned} &\text{(i)} \quad |\alpha_{1,m+1} - \alpha_{1,m}| < \varepsilon_1 \\ &\text{(ii)} \quad |O(\alpha_{1,m+1}) - O(\alpha_{1,m})| < \varepsilon_2 \quad . \end{aligned} \tag{30}$$

The search procedure continues until the termination criteria are met, which in words is as follows: (i) The movement in successive step sizes of α_1 is $<\varepsilon_1$ and (ii) the objective function is changing by an amount $<\varepsilon_2$. Typical values used for these two stopping tolerances are on the order of 10^{-5} and seem reasonable in light of the magnitude of the parameter being estimated ($\approx$2.8) and the value of the objective function in the vicinity of the found ML solution $O(\alpha_{\mathrm{ML}})$, of the order of magnitude 10^5 when E_1 is taken to be anywhere between 10 and 30 TeV, so the number of terms in the sum is between 182,000 to 26,000, respectively. Furthermore, changing ε_1 and/or ε_2 in either direction by an order of magnitude provided no noticeable change in results.

Figure 5 shows the ML estimates of α_1 for a zero-percent resolution detector obtained from equation (14) in comparison with the ML estimates obtained from a 40-percent resolution detector and applying the downhill simplex algorithm to equation (29) for 30 missions. This very close comparison suggests that the GCR event statistics are the dominating component of uncertainty in the estimation of the spectral parameter α_1.

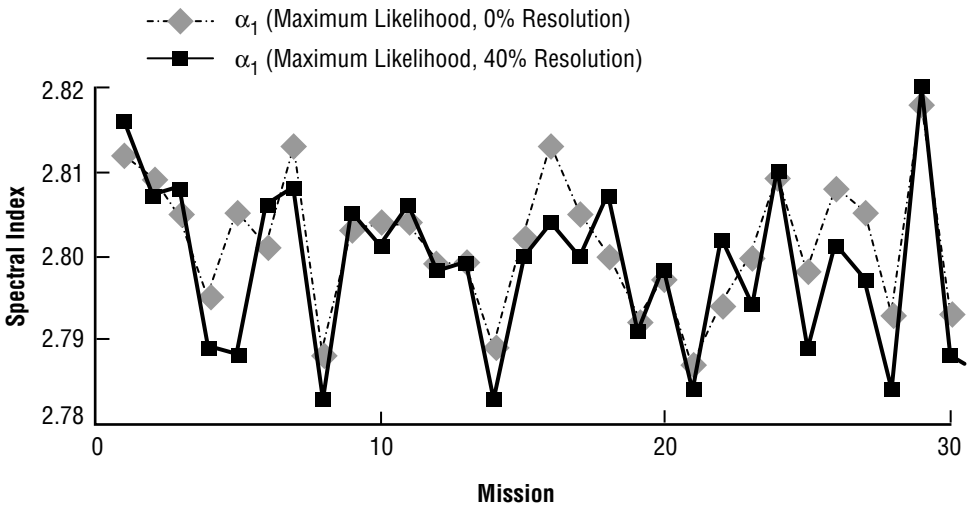

Figure 5. Maximum likelihood estimates for zero- and 40-percent resolution detector for 30 missions.

7. NON-GAUSSIAN DETECTOR RESPONSE FUNCTION

The results so far have assumed a Gaussian detector response function. While reference 4 suggests that a Gaussian function is reasonable, there is concern that perhaps the response function is skewed slightly to the right and that this "tail" will contribute to greater difficulties in estimating the spectral parameter. The gamma response function, capable of describing a wide variety of shapes with right-hand skewness (outer curve from the right in fig. 6), was introduced to address this concern. Its parameters were set to provide a constant 40-percent energy resolution over the study range 20–5,500 TeV from which events having incident energy described by a simple power law with $\alpha_1 = 2.8$ were simulated. The number of these events was determined using the baseline detector collecting power.

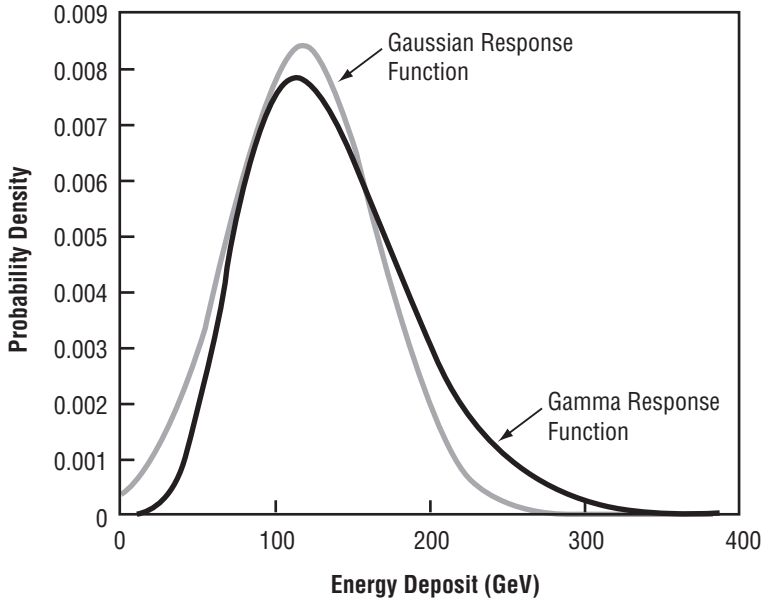

Figure 6. Gaussian and gamma detector response functions to 40 TeV proton (40-percent resolution).

Based on 10,000 simulated missions, the mean ML estimate of α_1 was 2.800 and standard deviation 0.0093 as compared to 2.800 and 0.0092 for the mean and standard deviation, respectively, corresponding to a Gaussian response function. Thus, the conclusion that this skewness and other non-Gaussian assumptions are insignificant when using the method of ML. However, as will be shown, the real key is not so much a matter of what the response function is as knowing what it is; i.e., an accurately understanding of the response function over the incident energy range must be made. It should also be noted that while the gamma response function as modeled has a constant energy resolution of 40 percent, the Gaussian used in this comparison had a 39-percent resolution as previously discussed.

8. ENERGY-DEPENDENT RESOLUTION STUDY

The situation in which the detector response function is assumed to be Gaussian, but its energy resolution varies with incident GCR event energy, is of particular interest to designers of cosmic-ray detectors. In the studies presented so far in this TP, the detector response function is assumed to be Gaussian with a linear mean response (energy deposit) of the form $(a + bE)$ and with constant detector energy resolution ρ so that the parameter σ in the Gaussian response function is defined as $\sigma(E) = \rho(a + bE)$. Two cases of interest are as follows: (1) Energy resolution is "getting better," from 40-percent resolution at E_1 = 20 TeV to 30 percent at E_2 = 5,500 TeV and (2) "getting worse," from 30-percent resolution at E_1 = 20 TeV to 40 percent at E_2 = 5,500 TeV. These two cases are modeled by assuming that $\sigma(E)$ is a linear function of incident GCR energy of the form $(c + dE)$ and then the coefficients c and d are determined by matching the conditions for each of the two cases. Doing so yields the energy-dependent resolution curves depicted in figure 7.

Table 1 shows the results based on 100 simulated missions using the same incident GCR energies for both cases. The mean estimates are seen as essentially unbiased with standard deviations having expected comparisons; e.g., standard deviations slightly larger for the "getting worse" case. The constant 30- and 40-percent cases are included for comparison.

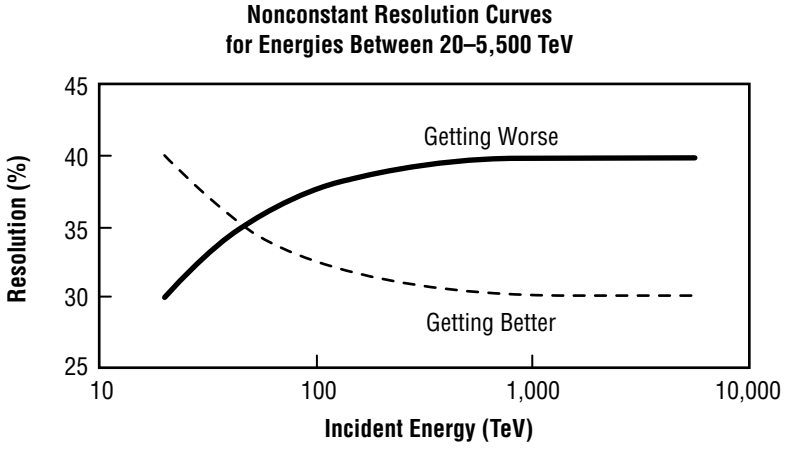

Figure 7. Energy-dependent resolution curves.

Table 1. Nonconstant energy resolution study.

Mean and Standard Deviation of the Maximum Likelihood Estimate of α_1 Based on 5,000 Missions								
Spectral Parameter	**Resolution**							
	Constant 30%		**Constant 40%**		**Nonconstant (Getting Better)**		**Nonconstant (Getting Worse)**	
	Mean	Std. Dev.	Mean	Std. Dev.	Mean	Std. Dev.	Mean	Std. Dev.
α_1	2.8	0.0088	2.8	0.0092	2.8	0.0090	2.8	0.0091

9. IMPLICATIONS OF DETECTOR RESPONSE MODEL UNCERTAINTIES

Maximum likelihood estimation of the spectral parameter α_1 using equation (29) requires the complete specificity of all detector response model parameters. The reality of knowing these parameters with little or no surrounding uncertainty depends largely on designers being able to calibrate the detector at different incident energies at a particle accelerator facility. However, because space-based detectors will be exposed to GCR events having energy much greater than those energies available at accelerator facilities, it becomes essential to gain an understanding of the detector's response function using Monte Carlo simulations of the detector's response (energy deposit) to those energies that cannot be attained at accelerator facilities. These simulations, coupled with a favorable comparison between simulation results and accelerator results at energies available in a test facility, will provide a better understanding of the detector response function.

Next, by way of example, an investigation is done of the impact on estimating α_1 when certain detector response function parameters are incorrectly known, and as shall be seen, this state of ignorance will manifest itself as a bias in the mean or point estimate of α_1. This state of ignorance is modeled by simulating detector responses according to one set of detector response function parameters and then using a different set of parameters in the detector response function g in equation (29) during the ML estimation procedure.

Since detector resolution is an important design parameter, consider first the case where the detector has a constant energy resolution. In an assumed state of misunderstanding, a different resolution value was used in equation (29). For example, suppose the real detector resolution is a constant 35 percent, but in the simplex search, the resolution parameter ρ is set to different constant values in equation (29), corresponding to resolutions ranging from 30 to 40 percent. This situation is modeled by simulating the detector responses Y_i as

$$Y_i = (a + bE_i)(1 + 0.35\, Z_i) \tag{31}$$

according to equation (17) and then set ρ to the different values in equation (29) in the ML procedure. The results for 500 simulated missions for each assumed resolution 30 through 40 percent while the "real" resolution is a constant 35 percent are presented in table 2. Note that the mean estimates exhibit a bias as a result of using incorrect values of ρ in equation (29). Note when $\rho = 0.35$ in equation (29) and hence matches the "real" resolution as used in equation (31) to simulate the detector responses, the means of the ML estimates match the assumed spectral parameter value of $\alpha_1 = 2.8$ used in the simulation.

Table 2. Biased estimate of α_1 when detector energy resolution is incorrectly known and assumed to be a constant 35 percent.

Real Energy Resolution	30%	31%	32%	33%	34%	35%	36%	37%	38%	39%	40%
Mean Estimate of α_1	2.83	2.83	2.82	2.81	2.81	2.80	2.79	2.79	2.78	2.77	2.76

Another interesting situation to consider is when the real detector resolution is energy dependent, but in a state of ignorance, a constant resolution value is used in equation (29) in the ML estimation of α_1. For example, if the real detector resolution is "getting better" as in figure 7 but instead a constant $\rho = 0.40$ is used in equation (29), a mean estimate of 2.81 for α_1 is obtained, whereas if $\rho = 0.35$ is used in equation (29), a mean estimate of 2.78 is obtained. One may initially be surprised by this comparison since 0.35 can roughly be considered the average resolution value for this energy-dependent case and that using a constant $\rho = 0.35$ in equation (29) should provide a closer result (less bias) than when ρ is set to 0.40. However, remember that the $\rho = 0.40$ assumption is closest to "reality" in the region where events are most numerous because of the steepness of the power law and the true energy-dependent case does start at 40-percent resolution. Also interesting is that if $\rho = 0.38$ in equation (29), the mean estimate 2.8 is obtained, even though the "real" resolution is the energy-dependent "getting better" case—a result discovered by trial and error!

A much larger bias in the estimate of α_1 is observed when the case where the real detector response function is the gamma function with a constant energy resolution of 40 percent, as depicted in figure 6, but instead, in a state of misunderstanding, a Gaussian response function in the ML procedure is assumed and the Gaussian response function defined in equation (18) is substituted into equation (29), resulting in a mean estimate of 2.52 for α_1.

10. APPLICATION TO REAL COSMIC-RAY DATA

In these simulations, the GCR events are simulated from an energy range E_1 to E_2, where typically $E_2 = 5{,}500$ TeV for this generic-sized detector and E_1 is a value between 5 and 25 TeV. The choice of E_2 is based on the collecting power of the detector and is chosen such that there will be only a negligible number of events above E_2. The selection of E_1 is largely dictated by the practical number of events that can be handled in the simulation for several thousand missions.

Next, for each of these simulated GCR events, a detector response is simulated according to the assumed detector response function and then the full set of simulated responses are used to estimate the spectral parameters. However, because no energies below E_1 are simulated, frequency histograms of the simulated detector responses do not match the front-end portion of a real cosmic-ray energy spectrum. This difference or mismatch is an artifact of not having generated events from below E_1 that would have had the effect of filling in this front-end portion of the histogram and for consequently resembling a real cosmic-ray energy spectrum.

This difference is not critical when making relative comparisons of the effects of design parameters when the detector response function parameters used to generated the simulated responses match those detector response function parameters used in equation (29) in the simplex search for the ML estimate of α_1; i.e., a perfect understanding is had of the detector response function. However, when the impacts of response function uncertainties are investigated, it is more important that the simulation techniques produce results that are closer to a real cosmic-ray energy response spectrum.

To make the histogram of the simulated detector responses look like a real cosmic-ray energy spectrum, a cut y_c in the simulated detector responses is introduced and all energy deposits smaller than y_c are dropped. In the simulation, the choice of y_c dictates admissible values of E_1 because E_1 must be chosen so that only a negligible number of events having incident energy $<E_1$ deposit energies $>y_c$, which of course depends on the detector's energy resolution. For example, if $y_c = 80$ GeV corresponding to the mean energy deposit of a 25-TeV GCR event and a Gaussian response function having 40-percent energy resolution and mean response $(a + bE)$ is considered, as used for the baseline detector and defined in equation (18), then E_1 can be any value $\leq$10 TeV, since only a negligible number of events from below 10 TeV will deposit more than 60 GeV. Selecting $E_1 = 10$ TeV provides $\approx 182{,}000$ GCR events and setting $y_c = 80$ GeV and dropping all simulated detector responses smaller than y_c leaves $\approx 44{,}500$ events on average above y_c, which produces a simulated response spectrum that does indeed resemble a real response spectrum. Table 3 shows the average number of events with energy deposits $>y_c$ for selected values of E_1 from 2 to 20 TeV. The practical benefit of table 3 is that it provides the optimal value to set E_1 in the simulation for a given cut y_c so as to minimize the number of events to initially simulate and achieve the same result. For example, if the cut is set at 60 GeV, then $E_1 = 4$ TeV would be set, since there is no additional benefit by taking $E_1 < 4$ TeV.

Table 3. Number of simulated energy deposits above cut y_c for various E_1 for Gaussian detector response function with 40-percent resolution.

	Cut y_c (GeV)	54	59	67	75	80	93	106
$N_0(>E_1)$	E_1 (TeV)							
3,293,737	2	127,707	97,784	69,979	52,896	44,873	31,487	23,440
1,587,539	3	127,605	97,828	70,013	52,906	44,878	31,487	23,465
945,876	4	126,796	97,648	69,936	52,846	44,837	31,468	23,434
632,988	5	124,971	97,196	69,901	52,841	44,812	31,451	23,424
455,899	6	121,685	96,151	69,731	52,820	44,808	31,447	23,414
345,433	7	116,887	94,211	69,358	52,747	44,779	31,426	23,407
271,630	8	110,969	91,438	68,644	52,621	44,769	31,461	23,427
219,737	9	104,270	87,799	67,457	52,313	44,646	31,440	23,407
181,777	10	97,235	83,592	65,793	51,766	44,412	31,416	23,389
153,119	11	90,162	78,980	63,680	50,982	44,073	31,404	23,427
130,921	12	83,311	74,209	61,201	49,866	43,463	31,313	23,418
113,354	13	76,840	69,427	58,464	48,500	42,658	31,146	23,381
99,198	14	70,819	64,801	55,625	46,941	41,688	30,907	23,352
87,613	15	65,292	60,377	52,713	45,202	40,518	30,576	23,286
78,004	16	60,242	56,217	49,817	43,357	39,237	30,138	23,165
69,939	17	55,655	52,371	47,008	41,454	37,823	29,583	23,003
63,101	18	51,465	48,748	44,292	39,562	36,396	28,967	22,785
57,249	19	47,714	45,464	41,707	37,678	34,923	28,276	22,528
52,200	20	44,320	42,451	39,295	35,835	33,436	27,510	22,206

A very important benefit is realized by introducing the cut y_c; that is, the lower limit of integration in equation (29) can be set to any value $E_L < E_1$ with the implication that this ML procedure can be made independent of the range of integration, as long as E_L is chosen wisely using table 3 (or its equivalent for detectors having a different energy resolution), so that the ML estimation procedure herein developed can now be applied to real cosmic-ray detector response data. It should be noted that cuts on the high end are not necessary to consider since any value $E_H \geq E_2$ is suitable because the number of events above E_2 is negligible and so ϕ_0 is approximately zero when $E > E_2$ in the integral definition of the detector response pdf. However, setting E_H unnecessarily high would result in many unnecessary calculations in the numerical integration of equation (29).

Introduction of a cut y_c requires a modification to the objective function in equation (29) to handle the conditional detector response distribution because of the constraint y > y_c. Thus, the objective function using cut y_c becomes

$$O(\alpha_1) = -\log L = -\sum_{j=1}^{N} \log\left[g_0\left(y_j \mid y_j > y_c; \alpha_1\right)\right] , \tag{32}$$

where

$$g_0(y_j \mid y_j > y_c;\alpha_1) = \frac{\int_{E_L}^{E_H} g(y_j \mid E;\rho)\,\phi_0(E;\alpha_1)dE}{1 - \int_0^{y_c} g_0(y;\alpha_1)dy}, \quad y_j > y_c \ . \tag{33}$$

From a simulation point of view, E_1 = 2 TeV is about the lowest value that was used because of the vast number of generated events and the requirement to handle thousands of simulated missions necessary for meaningful inferences. Consequently, cuts much less than 60 GeV were not used in these studies. However, cuts in real cosmic-ray data can be taken to be much lower since the real spectrum is automatically filled in from events having incident energies much less than 2 TeV and the lower limit of integration can then be taken to be any small value.

11. CONFIDENCE INTERVAL FOR α_1

The ML estimate α_{ML} obtained from equation (29) was shown to (1) be unbiased, (2) attain the Cramer-Rao minimum variance bound, and (3) be normally distributed when the number of events N is ≈1,200 or larger. Thus, the variance of α_{ML} is $\text{Var}(\alpha_{ML}) = -1/[\partial^2 LL/\partial\alpha_1^2]$ evaluated at α_{ML} for any given "mission" and where LL denotes the log-likelihood function given in equation (28) which can readily be obtained by numerical methods. A confidence interval can then be constructed for the unknown spectral parameter α as illustrated for each of 20 missions at 95-percent confidence in figure 8.

Extending the number of simulated missions to 2,000 provides a frequency histogram of α_{ML} as shown in figure 9 and of the estimated standard deviation of α_{ML} as shown in figure 10.

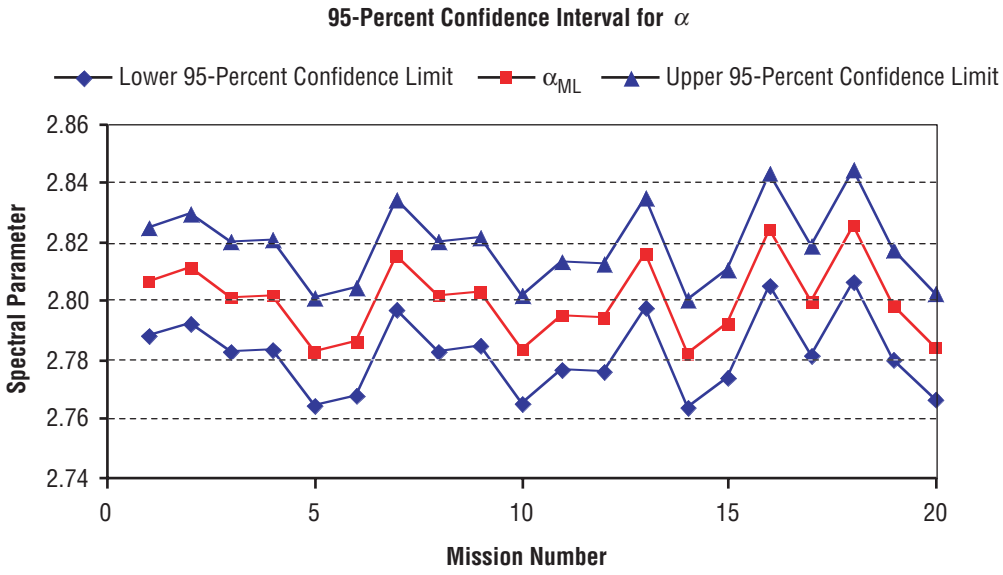

Figure 8. Maximum likelihood estimate with 95-percent confidence interval for 20 "missions."

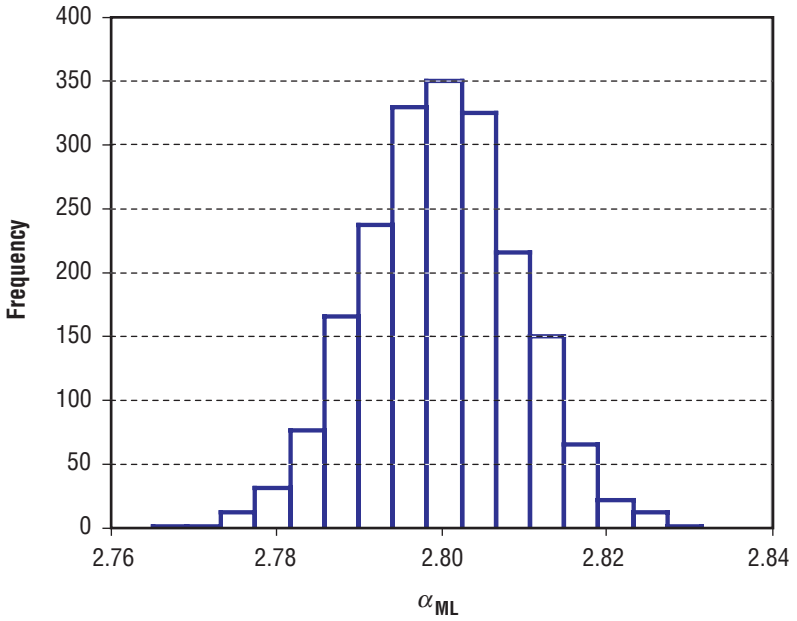

Figure 9. Frequency histogram of α_{ML} (2,000 missions).

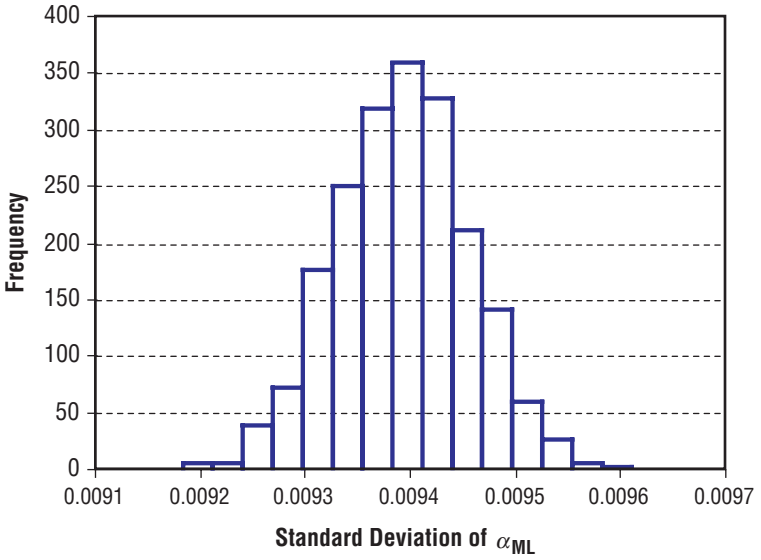

Figure 10. Frequency histogram of the estimated standard deviation of α_{ML} (2,000 missions).

12. TESTING FOR SLOPE DIFFERENCES OF TWO COSMIC-RAY ELEMENTAL SPECIES

Given two cosmic-ray elemental species A and B with slopes α and β, an important hypothesis to test is

H_0: $\alpha - \beta = 0$ (same "slopes")

versus

H_1: $\alpha - \beta \neq 0$.

To test this hypothesis, ML estimates α_{ML} and β_{ML} for each slope parameter using equation (29) and their respective variances Var(α_{ML}) and Var(β_{ML}), numerically obtained as discussed in section 11. Because α_{ML} and β_{ML} are both normally distributed for large N, the test statistic $T = (\alpha_{ML} - \beta_{ML})$ is used to test H_0. Note the following:

1. T has mean $\mu_T = (\alpha - \beta)$ because α_{ML} and β_{ML} are unbiased.
2. The standard deviation of T is $\sigma_T = \sqrt{\mathrm{Var}(\alpha_{ML}) + \mathrm{Var}(\beta_{ML})}$ because α_{ML} and β_{ML} are independent.
3. T is normally distributed because α_{ML} and β_{ML} follow the normal distribution.
4. T is normal(0, σ_T) when H_0 is true.

A two-sided test rejects H_0 with confidence C whenever $|T| > z_{c/2}\sigma_T$, where $z_{c/2}$ is the critical value of the normal distribution for confidence level C for a two-sided test. The width of the confidence interval for $(\alpha - \beta)$ is then $2\, z_{c/2}\sigma_T$.

Furthermore, if the number of events is doubled, then let D denote the test statistic similarly defined as T. Then D is normally distributed with mean zero and standard deviation σ_D under H_0 also; note that $\sigma_D = \sigma_T$ /Sqrt(2) since the variance of each ML estimate is halved when the number of events doubles as discussed in section 13. Thus, the width of the corresponding confidence interval is reduced by a factor of 1/Sqrt(2) when the number of events doubles.

13. SUMMARY, REMARKS, AND CONCLUSIONS

Two methods for estimating the single spectral index α_1 of a simple power law have been investigated. The first method, called the method of moments, was found to be very useful in studying the general nature of the statistical estimation problem as well as yielding an analytical solution that could be compared with Monte Carlo simulation results. Furthermore, when the detector resolution is better than 30 percent so that the truncation of the detector response function is negligible, the method of moments provides an estimator of α_1 without requiring specific knowledge of the detector resolution ρ but only that it is better than 30 percent. This does not imply ρ is insignificant when it is <30 percent, but only that the correction terms in equations (24)–(26) can be ignored. Thus, explicit knowledge of the value of ρ is not needed to estimate α_1. In fact, the standard deviation of the estimator increases as ρ increases, as one would expect, and results from the fact that whatever ρ happens to be, its impact is communicated to the estimate of α_1 through the variance of the detector mean response $\bar{Y}$—a function of ρ as indicated in equations (26)–(28). Another interesting result is that when the resolution is <30 percent, the explicit functional form of the detector model need not be known, but only that it is symmetric. Unfortunately, most detector response functions are worse than 30-percent resolution and may be asymmetric as well.

The method of ML estimation clearly stands out as the method of choice for estimating α_1 in terms of minimum variance and consistency (asymptotically unbiased) as well as asymptotic normality that allows for probabilistic statements, such as confidence intervals for the unknown spectral parameter. These results as a function of detector resolution are shown in figure 8.

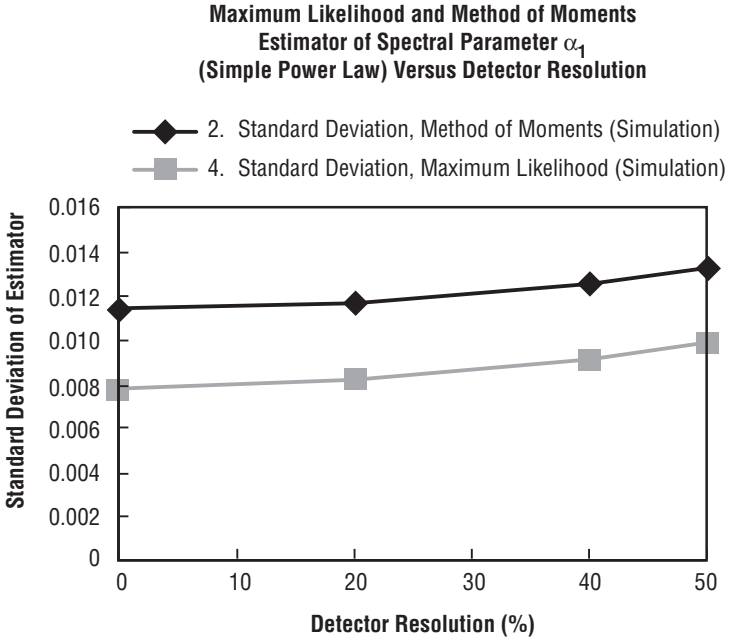

Figure 11. Comparison between method of moments and ML as a function of detector resolution.

When compared to the standard deviation of the method of moments estimator, the ratio varies from 1.47 for the zero-percent resolution detector to 1.33 for the 50-percent resolution detector, which is roughly equivalent to losing half of the detector's collecting power by choosing the inferior method of moments estimation technique.

Also shown is that the standard deviation of the estimate for both estimation procedures is inversely proportional to the square root of the sample size, so that halving the collecting power increases the standard deviation by a factor of $\sqrt{2}$. This holds true for the standard deviation of the ML estimate as long as it attains the Cramer-Rao lower bound, which it does when the number of GCR events exceeds 2,000.

Another important result is the relationship between the collecting power and the energy resolution of the detector. A measure of the detector's ability to estimate the spectral parameter α_1 is its standard deviation, as seen in figures 8 and 9. The dominant component of the standard deviation of α_{ML} is attributable directly to the large fluctuations in GCR incident energies, being driven by the large variance and other higher moments of the simple power law distribution. This large component can only be reduced by increasing the number of events *N* that is controlled by the collecting power of the detector. A comparison of the standard deviation of α_{ML} for the generic detector discussed in this TP and when its collecting power is halved is shown in figure 9. Table 4 provides the numerical results used to construct many of the figures in this section.

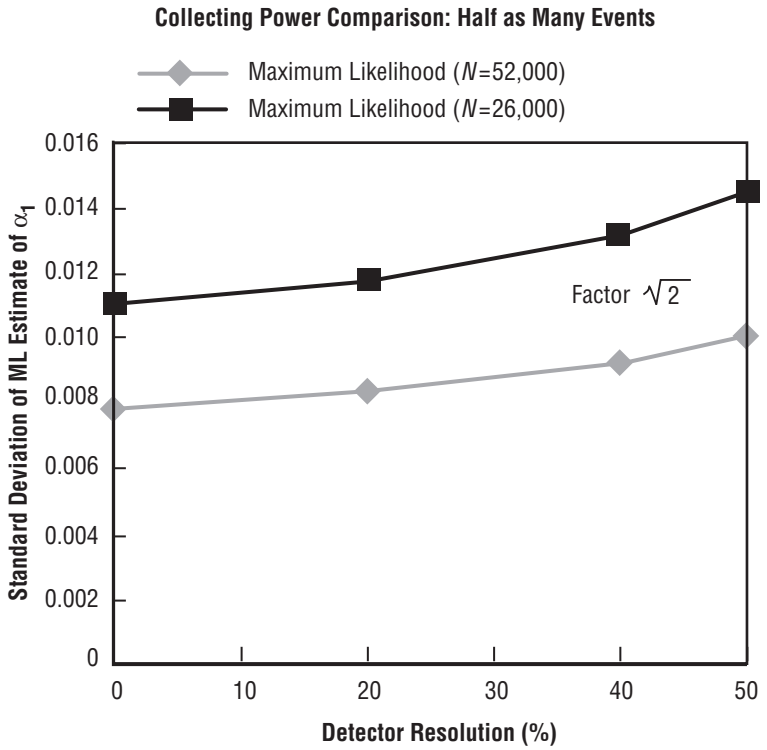

Figure 12. Comparing the effect of collecting power on the standard deviation of the ML estimate of the spectral index α_1.

Table 4. Numerical values used to construct figures 11 and 12 GCR.

E_1=20 TeV, E_2=5,500 TeV, α_1=2.8, $N_{average}$=52,000 Events. 5,000 Mission Averages for Simulation Results.	Detector Resolution			
	0%	20%	40%	50%
1. Method of moments (theory)	0.0115	0.0116	0.0128	0.0136
2. Method of moments (simulation)	0.0114	0.0117	0.0125	0.0133
3. Maximum likelihood (Cramer-Rao lower bound)	0.00786	Analytical solution not available		
4. Maximum likelihood (simulation)	0.0078	0.0083	0.0092	0.0100
5. Mean detector response (GeV) (theory)	130.66	130.66	131.58	138.85
6. Mean detector response (GeV) (simulation)	130.66	130.64	130.64	138.81
7. Standard deviation (theory)	192.07	197.61	213.69	239.77
8. Standard deviation (simulation)	191.47	196.86	213.33	238.82
9. Coefficient of variation V_Y (detector, %)	147	151	162	173
E_1=20 TeV, E_2=5,500 TeV, α_1=2.8, $N_{average}$=26,000 Events. 5,000 Mission Averages for Simulation Results.				
10. Maximum likelihood	0.0110	0.0118	0.0132	0.0144
11. Ratio of line 4 to line 10, compare to $\sqrt{2}$	1.41	1.42	1.43	1.44

REFERENCES

1. Sina, R.; and Seo, E.S.: "How Well Can a Cosmic Ray Spectral Kink be Measured?" *COSPAR 32*, Nayoya, Japan, 1998.

2. Kendall, M.G.; and Stuart, A.: *The Advanced Theory of Statistics*, Vol. 1, 2nd ed., Hafner Publishing Company, NY, p. 243, 1963.

3. Rheinfurth, M.; and Howell, L.W.: "Probability and Statistics in Aerospace Engineering," *NASA TP—1998–207194*, Marshall Space Flight Center, AL, 1998.

4. Lee, J.; Watts, J.; and Howell, L.: "Simulations of a Thin Sampling Calorimeter With GEANT/FLUKA," *J. Nuclear Instruments*, In press, 2001.

5. Harris, B., *Theory of Probability*, Addison-Wesley, Reading, MA, p. 128, 1966.

6. *Numerical Recipes in FORTRAN*, Cambridge University Press, New York, NY, p. 402, 1992.

REPORT DOCUMENTATION PAGE

Form Approved
OMB No. 0704-0188

1. AGENCY USE ONLY *(Leave Blank)*	2. REPORT DATE	3. REPORT TYPE AND DATES COVERED
	May 2001	Technical Publication

4. TITLE AND SUBTITLE
A Recommended Procedure for Estimating the Cosmic-Ray Spectral Parameter of a Simple Power Law With Applications to Detector Design

5. FUNDING NUMBERS

6. AUTHORS
L.W. Howell

7. PERFORMING ORGANIZATION NAMES(S) AND ADDRESS(ES)
George C. Marshall Space Flight Center
Marshall Space Flight Center, AL 35812

8. PERFORMING ORGANIZATION REPORT NUMBER
M–1015

9. SPONSORING/MONITORING AGENCY NAME(S) AND ADDRESS(ES)
National Aeronautics and Space Administration
Washington, DC 20546–0001

10. SPONSORING/MONITORING AGENCY REPORT NUMBER
NASA/TP—2001–210989

11. SUPPLEMENTARY NOTES
Prepared by Space Science Department, Science Directorate

12a. DISTRIBUTION/AVAILABILITY STATEMENT
Unclassified-Unlimited
Subject Category 90
Nonstandard Distribution

12b. DISTRIBUTION CODE

13. ABSTRACT *(Maximum 200 words)*

A simple power law model consisting of a single spectral index α_1 is believed to be an adequate description of the galactic cosmic-ray (GCR) proton flux at energies below 10^{13} eV. Two procedures for estimating α_1, the method of moments and maximum likelihood (ML), are developed and their statistical performance compared. It is concluded that the ML procedure attains the most desirable statistical properties and is hence the recommended statistical estimation procedure for estimating α_1. The ML procedure is then generalized for application to a set of real cosmic-ray data and thereby makes this approach applicable to existing cosmic-ray data sets.

Several other important results, such as the relationship between collecting power and detector energy resolution, as well as inclusion of a non-Gaussian detector response function, are presented. These results have many practical benefits in the design phase of a cosmic-ray detector as they permit instrument developers to make important trade studies in design parameters as a function of one of the science objectives. This is particularly important for space-based detectors where physical parameters, such as dimension and weight, impose rigorous practical limits to the design envelope.

14. SUBJECT TERMS
cosmic rays, simple power law energy spectrum, maximum likelihood, probability

15. NUMBER OF PAGES
44

16. PRICE CODE

17. SECURITY CLASSIFICATION OF REPORT	18. SECURITY CLASSIFICATION OF THIS PAGE	19. SECURITY CLASSIFICATION OF ABSTRACT	20. LIMITATION OF ABSTRACT
Unclassified	Unclassified	Unclassified	Unlimited